Secondary Bonding as a Force Dictating Structure and Solid-State Aggregation of the Primary Nitrene Sources (Arylsulfonylimino)iodoarenes ($ArINSO_2Ar'$)

Michelle Boucher,[†] Dainius Macikenas,[†] Tong Ren,[‡] and John D. Protasiewicz*,[†]

Contribution from the Departments of Chemistry, Case Western Reserve University, Cleveland, Ohio 44106-7078, and Florida Institute of Technology, Melbourne, Florida 32901

Received April 2, 1997[⊗]

Abstract: Iodonium ylides of the form $ArINSO_2Ar'$ (Ar = *m*-tolyl, Ar′ = *p*-nitrophenyl (**1**); Ar = *m*-tolyl, Ar′ = phenyl (**2**); Ar = *m*-tolyl, Ar′ = *p*-tolyl (**3**); Ar, Ar′ = *p*-tolyl (**4**)) have been prepared and crystallographically characterized. Comparisons to previously structurally characterized members of this class of materials (PhINTs (Ts = *p*-toluenesulfonyl), *o*-TolylINTs, MesINTs) demonstrate that apparently minor perturbations of the aromatic rings have substantial consequences on the supramolecular assemblies of these materials. The structures range from zigzag polymers (PhINTs, MesINTs), linear polymers (*o*-TolylINTs), layered structures (**1**), two-dimensional ladders (**2**, **3**, *o*-TolylINTs), to even three-dimensional stepladders (**4**). *Ab initio* calculations for a model molecule, $PhINSO_2Ph$, corroborate the presence of a I−N single bond and show considerable charges being localized on the I, N, S, and O atoms (+, −, +, and − charges, respectively). Extensive attractive networks of I···O and I···N secondary bonds thus dominate the solid-state polymers. Within the monomeric units of $ArINSO_2Ar'$, a U-turn-shaped motif is observed. This structural shape appears to optimize secondary bonding contacts between charged $INSO_2$ arrays. The structures of $ArINSO_2Ar'$ have been systematically characterized.

Introduction

Interest in the chemistry of organoiodine(III) continues to grow, with applications ranging from the engineering of molecular structures to organic and inorganic synthesis.[1−12] Organoiodine(III) species have unique properties and structures and are commonly described as hypervalent, owing to the increased valency of the iodine atom.[13] Iodosylbenzene (PhIO, $(PhIO)_n$) is, perhaps, the most widely known and utilized organoiodine(III) reagent. Not only does this readily prepared[14] reagent serve as a starting material for the synthesis of a wide variety of other organoiodine(III) species, but it also acts as an effective oxidant for many substrates.[15] Its oxidizing ability is greatly extended when it is used in conjunction with appropriate transition metal catalysts, and it also has found extensive applications as a primary oxo source for hydrocarbon oxidations and biomimetic studies.[16,17]

Nitrogen analogues of iodosylbenzene were first prepared in 1976 by the reaction of (diacetoxyiodo)arenes with *p*-toluenesulfonamide in methanol/water mixtures in the presence of base (eq 1).[18] These compounds are isolated as yellow, thermally

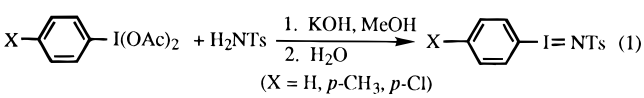

sensitive solids which are insoluble in nonreactive organic media. Also reported were reactions of the iodonium species with thioanisole, triphenylphosphine, and dimethyl sulfoxide to transfer the nitrene group from iodine to sulfur or phosphorus.

[†] Case Western Reserve University.
[‡] Florida Institute of Technology.
[⊗] Abstract published in *Advance ACS Abstracts,* September 15, 1997.

(1) Stang, P. J.; Zhdankin, V. V. *Chem. Rev.* **1996**, *96*, 1123−1178.
(2) Koser, G. F. In *The Chemistry of Halides, Pseudo-Halides and Azides, Supplement D2*; Patai, S., Rappoport, Z., Eds.; John Wiley & Sons: New York, 1995; pp 1173−1274.
(3) Varvoglis, A. *The Organic Chemistry of Polycoordinated Iodine*; VCH: New York, 1992.
(4) Oae, S.; Uchida, Y. *Acc. Chem. Res.* **1991**, *24*, 202−208.
(5) Moriarty, R. M.; Vaid, R. K.; Koser, G. F. *Synlett* **1990**, 365−383.
(6) Moriarty, R. M.; Vaid, R. K. *Synthesis* **1990**, 431−447.
(7) Moriarty, R. M.; Prakash, O. *Acc. Chem. Res.* **1986**, *19*, 244−250.
(8) Varvoglis, A. *Synthesis* **1984**, 709−726.
(9) Koser, G. F. In *The Chemistry of the Functional Groups, Supplement D*; Patai, S., Rappoport, Z., Eds.; John Wiley & Sons: New York, 1983; pp 721−811.
(10) Banks, D. F. *Chem. Rev.* **1966**, *66*, 243−266.
(11) Beringer, F. M.; Gindler, E. M. *Iodine Abs. Rev.* **1956**, *3*, 1−70.
(12) Sandin, R. B. *Chem. Rev.* **1943**, *32*, 249−276.
(13) Musher, J. I. *Angew. Chem., Int. Ed. Engl.* **1969**, *8*, 54−68.
(14) Saltzman, H.; Sharefkin, J. G. In *Organic Syntheses*; Baumgarten, H. C., Ed.; John Wiley & Sons: New York, 1973; Vol. 5, pp 658.
(15) Lead references for ArIO as oxo source: (a) Palucki, M.; Pospisil, P. J.; Zhang, W.; Jacobsen, E. N. *J. Am. Chem. Soc.* **1994**, *116*, 9333−9334. (b) Collman, J. P.; Zhang, X.; Lee, V. J.; Uffelman, E. S.; Brauman, J. I. *Science* **1993**, *261*, 1404−1411. (c) Ostovic, D.; Bruice, T. C. *Acc. Chem. Res.* **1992**, *25*, 314−320. (d) Zhang, W.; Loebach, J. L.; Wilson, S. R.; Jacobsen, E. N. *J. Am. Chem. Soc.* **1990**, *112*, 2801−2803. (e) McMurry, T. J.; Groves, J. T. In *Cytochrome P-450: Structure, Mechanism and Biochemistry*; Ortez de Montello, P. R., Ed.; Plenum Press: New York, 1986; pp 1−28 and references therein. (f) Guengerich, F. P.; Macdonald, T. L. *Acc. Chem. Res.* **1984**, *17*, 9−16.
(16) Holm, R. H.; Donahue, J. P. *Polyhedron* **1993**, *12*, 571−589.
(17) Holm, R. H. *Chem. Rev.* **1987**, *87*, 1401−1449.
(18) Yamada, Y.; Yamamoto, T.; Okawara, M. *Chem. Lett.* **1975**, 361−362.
(19) Some recent references for ArINR as nitrene source: (a) Lautens, M.; Klute, W.; Tam, W. *Chem. Rev.* **1996**, *96*, 49−92. (b) Harm, A. M.; Knight, J. G.; Stemp, G. *Tetrahedron Lett.* **1996**, *37*, 6189−6192. (c) Nishikori, H.; Katsuki, T. *Tetrahedron Lett.* **1996**, *37*, 9245−9248. (d) Shi, M.; Itoh, N.; Masaki, Y. *J. Chem. Res. (S)* **1996**, 352−353. (e) Takada, H.; Nishibayashi, Y.; Ohe, K.; Uemura, S. *J. Chem. Soc., Chem. Commun.* **1996**, 931−932. (f) Lim, B.-W.; Ahn, K.-H. *Synth. Commun.* **1996**, *26*, 3407−3412. (g) Li, Z.; Quan, R. W.; Jacobsen, E. N. *J. Am. Chem. Soc.* **1995**, *117*, 5889−5890. (h) Nishibayashi, Y.; Chiba, T.; Ohe, K.; Uemura, S. *J. Chem. Soc., Chem. Commun.* **1995**, 1243−1244. (i) Nishibayashi, Y.; Srivastava, S. K.; Ohe, K.; Uemura, S. *Tetrahedron Lett.* **1995**, *36*, 6725−6728. (j) Evans, D. A.; Faul, M. M.; Bilodeau, M. T. *J. Am. Chem. Soc.* **1994**, *116*, 2742−2753. (k) Li, Z.; Conser, K. R.; Jacobsen, E. N. *J. Am. Chem. Soc.* **1993**, *115*, 5326−5327. (l) Noda, K.; Hosoya, N.; Irie, R.; Ito, Y.; Katsuki, T. *Synlett* **1993**, 469−471. (m) Yang, R.-Y.; Dai, L.-X. *Synthesis* **1993**, 481−482.

S0002-7863(97)01048-2 CCC: $14.00

PhINTs (Ts = *p*-SO_2-C_6H_4-Me) has been extensively studied as a source of NTs groups in many reactions, with particular attention devoted to metal-catalyzed aziridinations and N-tosyliminations of olefins and alkanes.[19] Chiral aziridines are attractive materials for critical building blocks in organic syntheses.[20] Other iodine(III) reagents have also been developed to afford alkane N-functionalization.[21]

Mechanistic studies of atom or group transfer reactions using PhIO or PhINTs have been complicated by the insolubility of these materials in organic media, leaving many unanswered questions about their role in metal-catalyzed oxidations. In some cases, complexes containing the hypervalent iodine within the coordination sphere of the metal have been forwarded as intermediates, and, in a few, cases iodosylbenzene adducts have been isolated (but not crystallographically characterized).[22−38]

It has been demonstrated that the high solubility of these two materials in methanol arises from solvolysis to form (dimethoxyiodo)benzene and either water or *p*-toluenesulfonamide (eqs 2 and 3).[39,40] An equilibrium constant $K_s = 0.7(1)$ at 27 °C was

$$\mathrm{PhI{=}O + MeOH \rightleftharpoons PhI(OMe)_2 + H_2O} \qquad (2)$$

$$\mathrm{PhI{=}NTs + MeOH \overset{K_s}{\rightleftharpoons} PhI(OMe)_2 + H_2NTs} \qquad (3)$$

determined for eq 3. The insolubility of these materials in other solvents presumably is the result of their solid-state polymeric nature. Such assumptions were corroborated by early IR investigations of PhIO.[41−44] A recent EXAFS investigation of PhIO yielded further insight to the structural details of the polymeric nature.[45] I−O and I···O distances of 2.04 and 2.38 Å, and an I−O···I angle of 114°, allowed the structure to be portrayed as shown below. A similar zig−zag polymer based on I−N···N aggregation for PhINTs was deduced from powder diffraction data.[45]

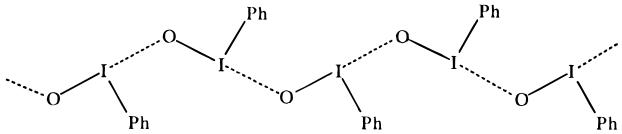

More recently, single-crystal X-ray data for PhINTs,[46,47] MesINTs,[46] and *o*-TolylINTs[48] have been reported. The structural data were most consistent with the presence of I−N single bonds. Each material displays extensive secondary bonding in the solid-state. Interestingly, these three compounds, differing only mildly in composition and intramolecular structure, yield four different supramolecular assemblies. As the reasons for such structural diversity were unclear, we sought to structurally characterize further crystalline derivatives containing differing substituents. An understanding of the factors which control the aggregation, and hence the insolubility, may also lead to materials more amenable for studies of nitrene transfer reactions and which may show greater resistance to undesired metal-catalyzed hydrolysis. A recent study has demonstrated that replacing PhINTs with PhINNs (Ns = *p*-SO_2-C_6H_4-NO_2) in the Rh_2(II)-catalyzed aziridination of olefins gives improved yields (85% versus 59% for styrene), while the corresponding nitrene precursors, $PhINSO_2Me$ and $PhINSO_2$-*p*-C_6H_4OMe, yield no aziridine products.[49,50] Rates of cyclohexene oxidation by variously substituted iodosylarenes mediated by iron porphyrins show marked dependency on the primary oxo source.[38]

Herein we present four new single-crystal X-ray structural details for ArINSO$_2$Ar′ which outline two new supramolecular arrays.[51] Both natural and designed systems extensively use intermolecular hydrogen bonding to bring together molecules into an amazing wealth of three-dimensional structures recognized in areas such as host−guest complexes and molecular recognition. Secondary I···O and I···N bonds bear a considerable resemblance to intermolecular hydrogen bonds and, thus, may be expected to yield as many and, perhaps, similar and even new structural types. The current work embarks a dissection of the forces responsible for controlling aggregation of ArINSO$_2$Ar′ in the solid-state. We also present the analysis of electronic structure calculations of ArINSO$_2$Ar′ on the basis of *ab initio* calculation, which aid in illuminating the nature of the intramolecular bonding and the electronic origin for aggregation of these unusual species in the solid state.

Experimental Section

Compounds **1**−**4** were prepared according to literature protocol,[18] replacing $PhI(OAc)_2$ with *m*-TolylI$(OAc)_2$ (prepared by oxidation of *m*-iodotoluene by either sodium perborate in glacial acetic acid[52] or by

(20) Tanner, D. *Angew. Chem. Int. Ed. Engl.* **1994**, *33*, 599−619.
(21) See: Zhdankin, V. V.; Krasutsky, A. P.; Kuehl, C. J.; Simonsen, A. J.; Woodward, J. K.; Mismash, B.; Bolz, J. T. *J. Am. Chem. Soc.* **1996**, *118*, 5192−5197 and references within.
(22) Khenkin, A. M.; Hill, C. L. *J. Am. Chem. Soc.* **1993**, *115*, 8178−8186.
(23) Birchall, T.; Smegal, J. A.; Hill, C. L. *Inorg. Chem.* **1984**, *23*, 1910−1913.
(24) Smegal, J. A.; Schardt, B. C.; Hill, C. L. *J. Am. Chem. Soc.* **1983**, *105*, 3510−3515.
(25) Smegal, J. A.; Hill, C. L. *J. Am. Chem. Soc.* **1983**, *105*, 3515−3521.
(26) Smegal, J. A.; Hill, C. L. *J. Am. Chem. Soc.* **1983**, *105*, 2920−2922.
(27) Hill, C. L.; Schardt, B. C. *J. Am. Chem. Soc.* **1980**, *102*, 6374−6375.
(28) Nam, W.; Valentine, J. S. *J. Am. Chem. Soc.* **1990**, *112*, 4977−4979.
(29) Yang, Y.; Diederich, F.; Valentine, J. S. *J. Am. Chem. Soc.* **1990**, *112*, 7826−7828.
(30) Nam, W.; Valentine, J. S. *J. Am. Chem. Soc.* **1991**, *113*, 7449.
(31) Tai, A. F.; Margerum, L. D.; Valentine, J. S. *J. Am. Chem. Soc.* **1986**, *108*, 5006−5008.
(32) Volz, H.; Müller, W. *Lieb. Ann. Chem.* **1992**, 1097−1101.
(33) Traylor, T. G.; Marsters, J. C., Jr.; Nakano, T.; Dunlap, B. E. *J. Am. Chem. Soc.* **1985**, *107*, 5537−5539.
(34) Appleton, A. J.; Evans, S.; Smith, J. R. L. *J. Chem. Soc., Perkins Trans. 2* **1996**, 281−285.
(35) Inchley, P.; Smith, J. R. L. *J. Chem. Soc., Perkins Trans. 2* **1995**, 1579−1587.
(36) Leanord, D. R.; Smith, J. R. L. *J. Chem. Soc., Perkins Trans. 2* **1991**, 25−30.
(37) Nam, W.; Baek, S. J.; Liao, K. I.; Valentine, J. S. *Bull. Korean Chem. Soc.* **1994**, *15*, 1112−1118.
(38) Harden, G. J. *J. Chem. Soc., Perkins Trans. 2* **1995**, 1883−1887.
(39) Schardt, B. C.; Hill, C. L. *Inorg. Chem.* **1983**, *22*, 1563−1565.
(40) White, R. E. *Inorg. Chem.* **1987**, *26*, 3916−3919.
(41) Bell, R.; Morgan, K. J. *J. Chem. Soc.* **1960**, 1209−1214.
(42) Dasent, W. E.; Waddington, T. C. *J. Chem. Soc.* **1960**, 2429−2432.
(43) Dasent, W. E.; Waddington, T. C. *J. Chem. Soc.* **1960**, 3350−3356.
(44) Siebert, H.; Handrich, M. *Z. Anorg. Allg. Chem.* **1976**, *426*, 173−183.
(45) Carmalt, C. J.; Crossley, J. G.; Knight, J. G.; Lightfoot, P.; Martin, A.; Muldowney, M. P.; Norman, N. C.; Orpen, A. G. *J. Chem. Soc., Chem. Commun.* **1994**, 2367−2368.
(46) Mishra, A. K.; Olmstead, M. M.; Ellison, J. J.; Power, P. P. *Inorg. Chem.* **1995**, *34*, 3210−3214.
(47) Protasiewicz, J. D. *Acta. Crystallogr. C* **1996**, 1570−1572.
(48) Cicero, R. L.; Zhao, D.; Protasiewicz, J. D. *Inorg. Chem.* **1996**, *35*, 275−276.
(49) Müller, P.; Baud, C.; Jacquier, Y. *Tetrahedron* **1996**, *52*, 1543−1548.
(50) Müller, P.; Baud, C.; Jacquier, Y.; Moran, M.; Nägeli, I. *J. Phys. Org. Chem.* **1996**, *9*, 341−347.
(51) Lehn, J.-M. *Supramolecular Chemistry*; VCH: New York, 1995.
(52) McKillop, A.; Kemp, D. *Tetrahedron* **1989**, *45*, 3299−3306.

Table 1. Crystal Data and Structure Refinement for **1**−**4**

	1	**2**	**3**	**4**
empirical formula	$C_{13}H_{11}IN_2O_4S$	$C_{14}H_{14}INO_2S$	$C_{13}H_{12}INO_2S$	$C_{14}H_{14}INO_2S$
formula weight	418.20	387.22	373.20	387.22
temperature (K)	293(2)	293(2)	293(2)	293(2)
wavelength (Å)	0.710 73	0.710 73	0.710 73	0.710 73
crystal system	monoclinic	monoclinic	monoclinic	monoclinic
space group	*C*2/*c*	$P2_1$	$P2_1/c$	$P2_1/n$
unit cell dimens				
a (Å)	32.414(3)	8.391(1)	7.2063(7)	15.155(1)
b (Å)	6.4440(8)	7.0264(8)	11.062(1)	6.2541(5)
c (Å)	14.112(1)	12.479(1)	16.660(2)	15.240(1)
β (deg)	$\beta = 102.723(8)°$	$\beta = 106.005(7)°$	$\beta = 100.613(7)°$	$\beta = 101.895(5)°$
vol (A^3)	2875.2(5) $Å^3$	707.21(13) $Å^3$	1305.4(2) $Å^3$	1413.4(2) $Å^3$
Z	8	2	4	4
density (calcd mg/mm^3)	1.932	1.818	1.899	1.820
absorption coeff (mm^{-1})	2.389	2.408	2.606	2.410
F(000)	1632	380	728	760
crystal size (mm)	0.28 × 0.24 × 0.14	0.22 × 0.24 × 0.14	0.30 × 0.12 × 0.12	0.42 × 0.16 × 0.08
crystal color	yellow	yellow	yellow	yellow
θ range for data collection (deg)	2.58−24.99	2.53−23.99	2.22−23.99	2.13−23.96
limiting indices	$-1 < h < 38$ $-1 < k < 7$ $-16 < l < 16$	$-1 < h < 9$ $-1 < k < 8$ $-14 < l < 14$	$-1 < h < 8$ $-1 < k < 12$ $-19 < l < 19$	$-1 < h < 17$ $-1 < k < 7$ $-17 < l < 17$
reflectns collected	3206	1731	2658	2994
independent reflectns	2539 ($R_{int} = 0.0485$)	1419 ($R_{int} = 0.0176$)	1901 ($R_{int} = 0.0771$)	2205 ($R_{int} = 0.0294$)
refinement method	full-matrix least-squares on F^2	full-matrix least-squares on F^2	full-matrix least-squares on F^2	full-matrix least-squares on F^2
data/restraints/params	2539/0/222	1419/1/215	1901/0/163	2205/0/205
goodness-of-fit on F^2	1.173	1.062	1.128	1.242
final *R* indices [$I > 2\sigma(I)$]	$R_1 = 0.0412$ $wR_2 = 0.1061$	$R_1 = 0.0209$ $wR_2 = 0.0532$	$R_1 = 0.0533$ $wR_2 = 0.1343$	$R_1 = 0.0301$ $wR_2 = 0.0701$
R indices (all data)	$R_1 = 0.0452$ $wR_2 = 0.1107$	$R_1 = 0.0218$ $wR_2 = 0.0539$	$R_1 = 0.0719$ $wR_2 = 0.1495$	$R_1 = 0.0437$ $wR_2 = 0.0754$
absolute structure parameter	na[a]	0.02(3)	na	na

[a] Not applicable.

oxidation with peracetic acid[53]) using the requisite arylsulfonamide in methanol. All of these materials decompose vigorously upon melting. We note that a sample of a highly insoluble material we believed to be *p*-$TsNIC_6H_4INTs$ (prepared from *p*-$(O_2CCF_3)_2IC_6H_4I(O_2CCF_3)_2$) loudly (during a routine melting point determination) at its decomposition temperature of about 95 °C; thus, care should be excercised in handling these materials at elevated temperatures.

***m*-TolylINSO$_2$-*p*-NO$_2$C$_6$H$_4$ (1):** ^{1}H NMR (300 MHz, DMSO-d_6) δ 8.03 (d, J = 8.8 Hz, 2H), 7.70 (d, J = 8.9 Hz, 2H), 7.52 (d, J = 7.4 Hz, 1H), 7.37 (s, 1H), 7.19−7.11 (m, 2H), 2.14 (s, 3H); FT-IR (Nujol) ν 1605(m), 1584(w), 1561(w), 1527(s), 1400(w), 1343(s), 1312(w), 1262(s), 1171(w), 1121(s), 1073(s), 1010(m), 989(m), 881(s), 851(s), 786(w), 769(s), 747(s), 734(s), 684(m), 678(s), 655(w), 628(s), 617(s), 600(s), 550(s); mp 130−132 °C dec.

***m*-TolylINTs (2):** ^{1}H NMR (300 MHz, DMSO-d_6) δ 7.50 (d, J = 7.7 Hz, 1H), 7.42 (d, J = 8.1 Hz, 2H), 7.29−7.14 (m, 3H), 7.05 (d, J = 8.1 Hz, 2H), 2.26 (s, 3H), 2.18 (s, 3H); FT-IR (Nujol) ν 1592(m), 1557(w), 1538(w), 1505(w), 1489(w), 1348(w), 1308(w), 1289(w), 1262(s), 1182(w), 1127(s), 1077(s), 1016(w), 987(m), 914(w), 890(s), 872(m), 850(w), 823(m), 797(w), 773(s), 733(w), 709(m), 668(s); mp 97−98 °C dec.

***m*-TolylINSO$_2$Ph (3):** ^{1}H NMR (300 MHz, DMSO-d_6) δ 7.60−7.49 (m, 3H), 7.40 (s, 1H), 7.35−7.25 (m, 3H), 7.20−7.11 (m, 2H); FT-IR (Nujol) ν 1592(m), 1557(m), 1340(w), 1262(s), 1161(m), 1127(s), 1075(s), 1023(w), 990(m), 872(s), 820(w), 784(m), 766(m), 686(m), 637(s); mp 83−88 °C dec.

***p*-TolyINTs (4):** ^{1}H NMR and mp were consistent with literature values.[18]

X-ray Crystallography. Yellow crystals of **1**−**4** were grown by slow cooling of methanol/water solutions of **1**−**4** at 7 °C.

Data Collection and Reduction. Data were collected with a Siemens P4 diffractometer (Mo Kα radiation, λ = 0.710 73 Å). Crystals were glued at the end of a glass fiber. Crystals were judged to be acceptable on the basis of ω scans and rotation photography. A random search located reflections to generate reduced primitive cells, and cell lengths were corroborated by axial photography. Additional reflections with 2θ values between 24.5 and 25° were appended to the reflection arrays and yielded the refined cell constants. Monoclinic unit cells were confirmed by further examination on the diffractometer, and final cell constants are presented in Table 1. Data for **1**−**4** were collected as presented in Table 1 and were corrected for absorption (empirical ψ scan).

Determination and Refinement of Structures. Direct methods (Siemens SHELXTL PLUS, Version 5.1) revealed all of the non-hydrogen atoms for **1**−**4**. All non-hydrogen atoms were refined anisotropically for **1**−**4** and the final least-squares refinement for each structure converged at the *R*-factors reported in Table 1. Full crystallographic details for **1**−**4** have been provided as Supporting Information.

1. The systematic absences were in agreement with *C*2/*c* or *Cc*, with successful refinement occurring only in the former space group. Hydrogen atoms for all carbons except C7 were located and refined at 1.2 B_{eq} of attached carbon atoms. Hydrogen atoms for C7 were generated at idealized positions with common isotropic thermal parameters.

2. The systematic absences were in agreement with $P2_1$. All hydrogen atoms were successfully located and refined at 1.2 B_{eq} of attached carbon atoms. Refinement of the other enantiomorph of **2** resulted in higher *R* values ($R_1 = 0.0235$, $wR_2 = 0.0653$, GOF = 1.205) and higher absolute structure factor (0.50(3)).

3. The systematic absences were in agreement with only $P2_1/c$. All hydrogen atoms for **3** were generated at idealized positions and refined with common isotropic thermal parameters.

4. The systematic absences were in agreement with only $P2_1/n$. Hydrogen atoms for all carbons except C14 were located and refined at 1.2 B_{eq} of attached carbon atoms. Hydrogen atoms for C14 were generated at idealized positions and refined with common isotropic thermal parameters.

Computational Procedure. *Ab initio* calculation at the 3-21G* level for model compound $PhINSO_2Ph$ was performed with the SPARTAN

(53) Sharefkin, J. G.; Saltzman, H. In *Organic Syntheses*; Baumgarten, H. C., Ed.; John Wiley & Sons: New York, 1973; Vol. 5, pp 660−662.

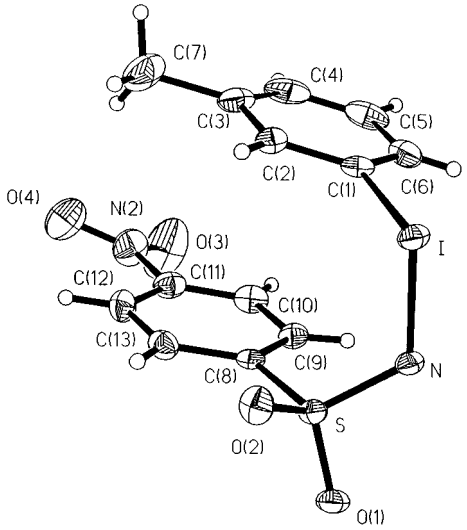

Figure 1. Thermal ellipsoid plot for the monomeric unit of *m*-TolylINSO$_2$-*p*-nitrophenyl (**1**).

package on a Silicon Graphics Indy platform.[54] Both the geometric parameters (bond lengths and angles, and some dihedral angles) for the Ph−I−N−SO$_2$−Ph core and the orientation of the phenyl groups were adapted from the X-ray structure of MesINTs, while a typical rigid hexagon shape (C−C and C−H are set at 1.40 and 1.05 Å, respectively) was assumed for both phenyl groups. Upon the completion of SCF calculation, both the formation of a covalent bond between atomic centers and the formal charge on individual atomic centers were analyzed by the built-in natural bond orbital and Mülliken charge partitioning modules.[54−56]

Results

Analogues of PhINTs with varying substituents were prepared according to eq 1. These materials were dissolved in MeOH (utilizing equilibrium formation of ArI(OMe)$_2$, eq 3), to which varying amounts of H_2O were added, and then chilled to 7 °C to promote formation of single crystals of ArINSO$_2$Ar′. After screening a number of these materials for crystallinity, we succeeded in obtaining four species suitable for X-ray diffraction studies: *m*-TolylINSO$_2$-*p*-NO$_2$C$_6$H$_4$ (**1**), *m*-TolylINTs (**2**), *m*-TolylINSO$_2$C$_6$H$_5$ (**3**), and *p*-TolylINTs (**4**). These four species allow for a systematic study of the nature of substituent effects on aromatic residues of both regions of ArINSO$_2$Ar′.

Figure 1 shows the structure obtained for the monomeric unit of **1**, and Table 2 lists important bond distances and angles. Within the monomer, I−N and I−C distances of 2.012(3) and 2.107(3) Å are found. A C−I−N bond angle of 99.3(1)° is consistent with an incipient T-shaped geometry upon accepting an intermolecular contact to an electronegative ligand. The two aromatic residues are nearly coplanar with the angle between the least-squares planes for each set of aromatic carbon atoms equal to 6.1(2)°. The centroid-to-centroid distance between aromatic rings is 3.591 Å in **1**.[57] One long intramolecular I···O contact of 3.278 Å between I and O2 is also observed.

The monomers of **1** aggregate in the solid-state to form a ruffled layered polymeric structure, as depicted in Figures 2 and 3. Surprisingly, the nitro groups do not participate in formation of the supramolecular architecture of **1**, as has been found in many other nitroiodoarenes.[58] Instead, the molecules are united by I···O (2.971, 3.361 Å) and I···N (3.073 Å) secondary bonds. The sheets of **1** are insulated from one another by layers of the *m*-methyl and *p*-nitro groups. The *m*-tolyl group of one unit of **1** has a near approach of the *p*-nitrophenyl group on one side of the layer (4.62 Å). The geometry at the iodine center of **1** (and **2**−**4**), including consideration of secondary bonds to iodine, will be discussed collectively below.

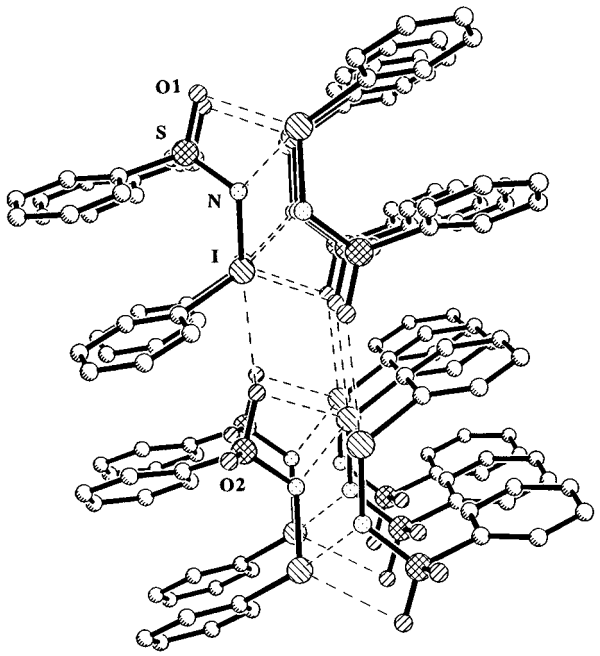

Figure 2. Solid-state aggregation of **1** as viewed down the *c* axis, polymeric sheets running parallel to the *b* axis. Hydrogen atoms, methyl groups, and nitro groups have been omitted for clarity.

Table 2. Selected Bond Distances and Angles for **1**−**4**

	1	**2**	**3**	**4**
		Distances (Å)		
I−N	2.012(3)	2.005(5)	1.997(8)	2.009(4)
I−C(1)	2.104(4)	2.104(5)	2.101(8)	2.113(4)
N−S	1.589(3)	1.610(5)	1.611(7)	1.622(4)
S−O(2)	1.439(3)	1.442(6)	1.447(8)	1.444(3)
S−O(1)	1.454(3)	1.446(5)	1.439(7)	1.429(3)
S−C(8)	1.791(4)	1.777(5)	1.778(7)	1.789(5)
		Angles (deg)		
N−I−C(1)	99.30(1)	100.8(2)	100.6(3)	102.1(2)
S−N−I	114.6(2)	111.3(3)	116.4(4)	114.4(2)
O(2)−S−O(1)	117.2(2)	116.5(4)	117.6(5)	116.6(2)
O(2)−S−N	116.1(2)	103.5(3)	104.2(4)	114.7(2)
O(1)−S−N	103.8(2)	114.4(3)	114.9(5)	103.5(2)
O(2)−S−C(8)	105.5(2)	108.1(3)	106.4(4)	106.5(2)
N−S−C(8)	107.6(2)	108.0(3)	105.8(4)	107.2(2)
O(1)−S−C(8)	106.0(2)	106.0(3)	107.2(4)	107.8(2)

Figure 4 reveals the details of the local environment for **2**. Table 2 lists important bond distances and angles. I−N and I−C distances of 2.005(5) and 2.104(5) Å closely resemble the corresponding values obtained for **1**. The C−I−N angle about the hypervalent iodine center is 100.8(2)°. The intramolecular centroid-to-centroid distance is 4.739 Å between the aromatic rings in **2**. The aromatic rings of **2**, by contrast to those of **1**, are substantially noncoplanar and describe an angle of 47.7(1)° between the residues.

(54) Spartan User's Guide,Version 3.0, 1993; Version 3.1, 1994, Wavefunction Inc., Irvine, CA,

(55) Mulliken, R. S. *J. Chem. Phys.* **1955**, *23*, 2343−2346 and references therein.

(56) Reed, A. E.; Weinstock, R. B.; Weinhold, F. *J. Chem. Phys.* **1985**, *83*, 735−746 and references therein.

(57) The centroid-to-centroid distances conviently describe the close contacts between two aromatic rings in cases where the two rings are not exactly coplanar (as is the case for all the compounds reported here). The centroid-to-centroid distances discussed can be intramolecular (between the Ar and Ar′ rings of one ArINSO$_2$Ar′ unit, Ar···Ar′) or intermolecular (between two ArINSO$_2$Ar′ units, either Ar···Ar, Ar···Ar′, or Ar′···Ar′).

(58) Desiraju, G. R. *Angew. Chem., Int. Ed. Engl.* **1995**, *34*, 2311−2327.

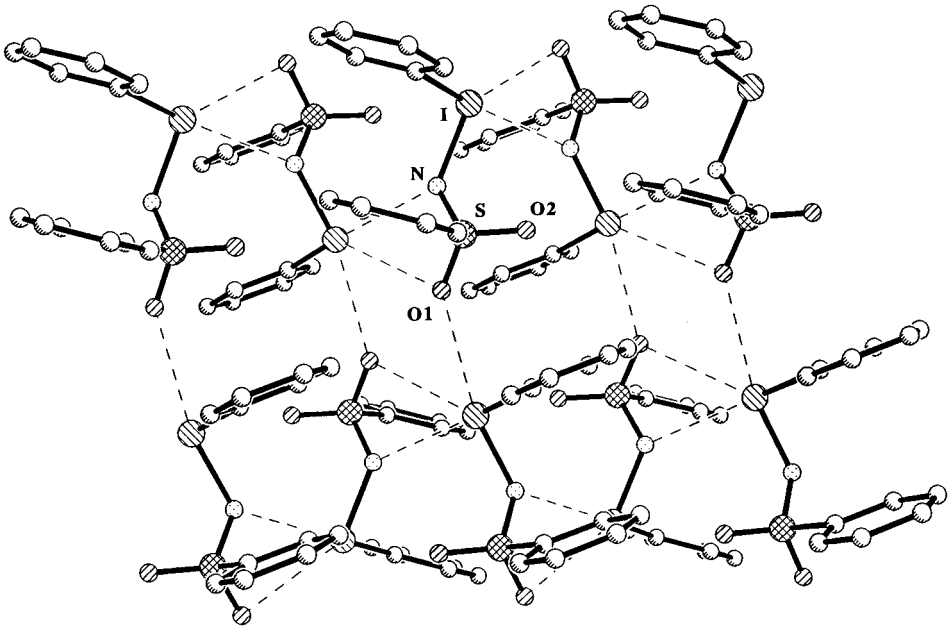

Figure 3. Solid-state aggregation of **1** as viewed down the *a* axis, polymeric sheets running parallel to the *b* axis. Hydrogen atoms, methyl groups, and nitro groups have been omitted for clarity.

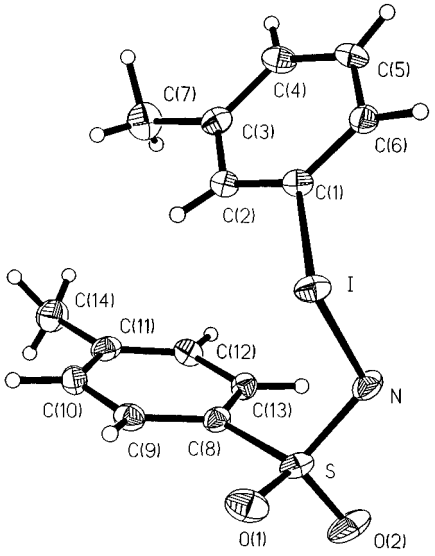

Figure 4. Thermal ellipsoid plot for the monomeric unit of *m*-Tolyl-$INSO_2$-*p*-tolyl (**2**).

Figure 5 describes the irregular ladder polymer formed by aggregation of the units of **2**. Both I···O (2.863 Å) and I···N (2.992 Å) secondary bonds are used to construct the polymer. Between the ladders, the aryl residues are somewhat interpenetrated and yield close Ar···Ar (4.60 Å) contacts. A similar structural arrangement is observed for *o*-TolylINTs and **3** (below).

Figure 6 displays the monomeric unit for **3**, and Table 2 lists important bond distances and angles. I−N and I−C distances are nearly the same as those for other members of the series, at 1.977(8) and 2.101(8) Å, respectively. Again, a value near 100° (100.6(3)°) is seen for the C−I−N bond angle. The two aromatic residues, like in the species presented above, lie somewhat above one another and feature a centroid-to-centroid distance of 3.60 Å. The rings are also nearly coplanar, having angles between the planes of the rings of 4.5(3)°.

Figure 7 illustrates the nature of the aggregation of **3** in the solid-state. The ladder-like structure formed is related to that observed for **2** and for the A polymorph of *o*-TolylINTs.

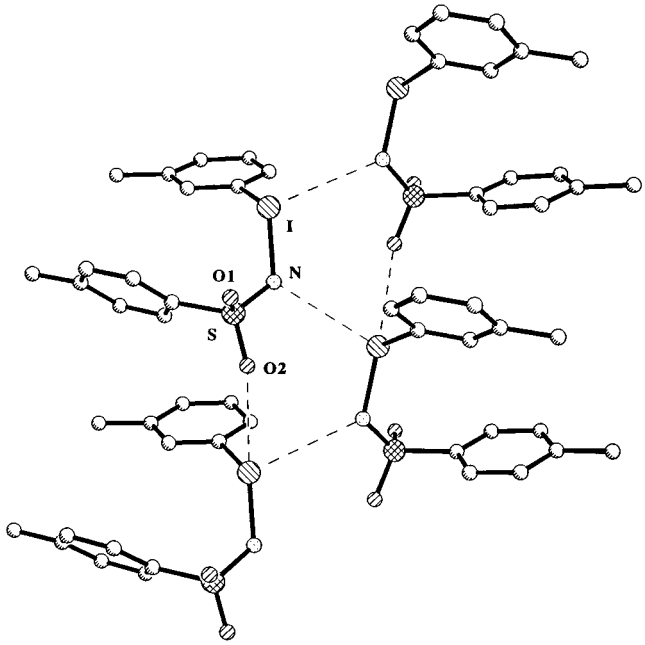

Figure 5. Solid-state aggregation of **2** as viewed down the *a* axis, polymeric ladders running parallel to the *b* axis. Hydrogen atoms have been omitted for clarity.

Compared to **2**, **3** uses rungs composed of shorter I···N (2.933 Å) and slightly longer I···O (3.250 versus 3.225 Å in **2**) secondary bonds, a probable ramification of the fact that the two rails of the ladder have slipped with respect to **2**. Along the rails the units are connected via I···O secondary bonds (2.975 Å).

The monomeric unit of **4** is portrayed in Figure 8 and Table 2 lists important bond distances and angles. As for other members of the $ArINSO_2Ar'$ series, an I−N distance close to 2.0 Å is observed (2.008(4) Å) and an I−C distance close to 2.1 Å (2.119(4) Å). The centroid-to-centroid distance is 3.819 Å for the aromatic rings in **4**; the centroids, like in the other $ArINSO_2Ar'$ complexes, are located upon one another. The aromatic rings of **4** shows some deviation from coplanarity and describe an angle of 11.6(2)° between the residues.

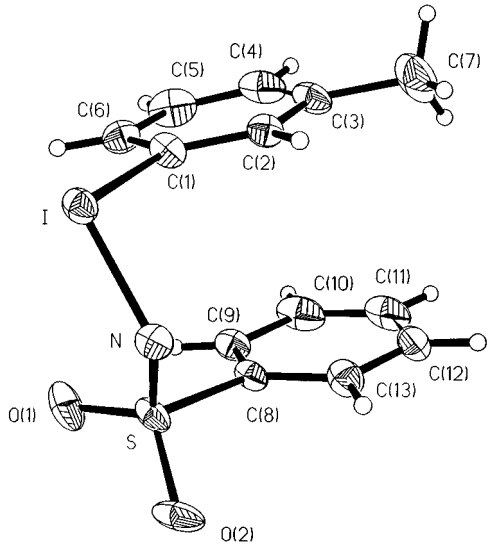

Figure 6. Thermal ellipsoid plot for the monomeric unit of *m*-TolylINSO$_2$-phenyl (**3**).

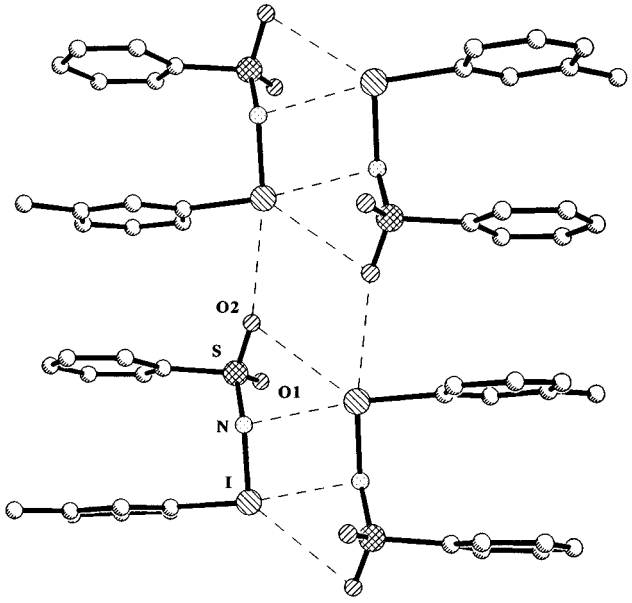

Figure 7. Solid-state aggregation of **3** with polymeric ladders running parallel to the *a* axis. Hydrogen atoms have been omitted for clarity.

In contrast to **1**−**3**, however, the nature of the aggregation of **4** is very different and unique (Figure 9). As opposed to the layered and ladder structures, the units of **4** have utilized secondary bonds to construct a molecular stairway or stepladder. Both I···O (3.191 ∼*trans* to N) and I···N (3.132 Å) secondary bonds are observed. The stepladder assembly may be related to the linear ladder observed for *o*-TolylINTs. In both structures, there exists very similar dimers of ArINSO$_2$Ar′ held together by I···N secondary bonds. The two structures differ by the nature of the I···O secondary bonds. In **4**, the sulfonyl oxygen atoms which are above and below the plane of the I and N atoms are engaged in forming I···O secondary bonds, whereas, in *o*-TolylINTs, the oxygen atoms in the plane of the I and N atoms are used to form such bonds. This differentiation is portrayed in Figure 10, with the similar units highlighted. Slightly longer secondary bonds are observed for **4**.

Discussion

The structural data for **1**−**4**, as presented above, in conjunction with published data for PhINTs, *o*-TolylINTs, and MesINTs, allow a detailed analysis and dissection of the bonding and aggregation of ArINSO$_2$Ar′.

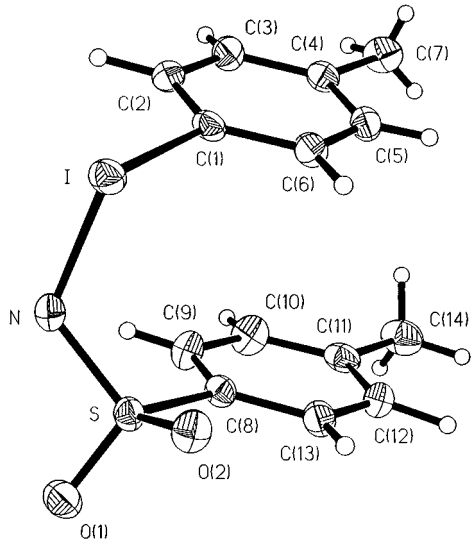

Figure 8. Thermal ellipsoid plot for the monomeric unit of *p*-TolylINSO$_2$-*p*-tolyl (**4**).

I−**N Bonding.** The key intramolecular features of the **1**−**4** and those of PhINTs, *o*-TolylINTs (polymorphs A and B), and MesINTs are summarized in Table 3. The I−N distance in all structures spans the narrow range of 1.997(8)−2.039(2) Å. The sum of the covalent radii for iodine (1.33 Å) and nitrogen (0.73 Å) predicts a I−N single bond distance of 2.06 Å. The I−N distances in ArINSO$_2$Ar′ can be compared to I−N distances of 2.06(2)−2.182(7) Å found for structurally characterized three-coordinate organoiodine(III).[59−62] Owing to the presence of a three-center, four-electron bond between the axial ligands and the iodine(III) centers, reduced bond orders and lengthened bonds are commonly observed. Species such as *N*-iodosuccinimide and *N*,*N*-diiodoformamide show I−N distances ranging from 2.049(8) to 2.100(7) Å.[63,64] Many linear two-coordinate iodine(I) structures have been characterized containing N−I−N arrays, and most of these materials show longer bond distances, ranging from 2.29 to 2.31 Å.[65]

Much discussion has centered on the importance of ionic contributions to bonding, and corrections for such effects have been forwarded by the Schomaker−Stevenson equation (eq 4),

$$r = r_1 + r_2 - \beta|\chi_1 - \chi_2| \qquad (4)$$

where r_1 and r_2 are covalent radii for the atoms, and $|\chi_1 - \chi_2|$ represents the absolute value of the difference in electronegativity for the two elements.[66−69] Different values for the β term have been forwarded, this term being largest for bonds to elements of the first row. Power and co-workers have dem-

(59) Naae, D. G.; Gougoutas, J. Z. *J. Org. Chem.* **1975**, *40*, 2129−2131.
(60) Prout, K.; Stevens, N. M.; Coda, A.; Tazzoli, V.; Shaw, R. A.; Demir, T. *Z. Naturforsch.* **1976**, *31b*, 687−688.
(61) Balthazor, T. M.; Godar, D. E.; Stults, B. R. *J. Org. Chem.* **1979**, *44*, 1447−1449.
(62) Zhdankin, V. V.; Krasutsky, A. P.; Kuehl, C. J.; Simonsen, A. J.; Woodward, J. K.; Mismash, B.; Bolz, J. T. *J. Am. Chem. Soc.* **1996**, *118*, 5192−5197.
(63) Padmanabhan, K.; Paul, I. C.; Curtin, D. Y. *Acta Crystallogr.* **1990**, *C46*, 88−92.
(64) Pritzkow, H. *Monatsh. Chem.* **1974**, *105*, 621−628.
(65) Brock, C. P.; Fu, Y.; Blair, L. K.; Chen, P.; Lovell, M. *Acta. Crystallogr.* **1988**, *C44*, 1582−1585.
(66) Schomaker, V.; Stevenson, D. P. *J. Am. Chem. Soc.* **1941**, *63*, 37−40.
(67) Pauling, L. *The Nature of The Chemical Bond*, 3rd ed.; Cornell University Press: Ithaca, NY, 1960.
(68) Blom, R.; Haaland, A. *J. Mol. Struct.* **1985**, *128*, 21−27.

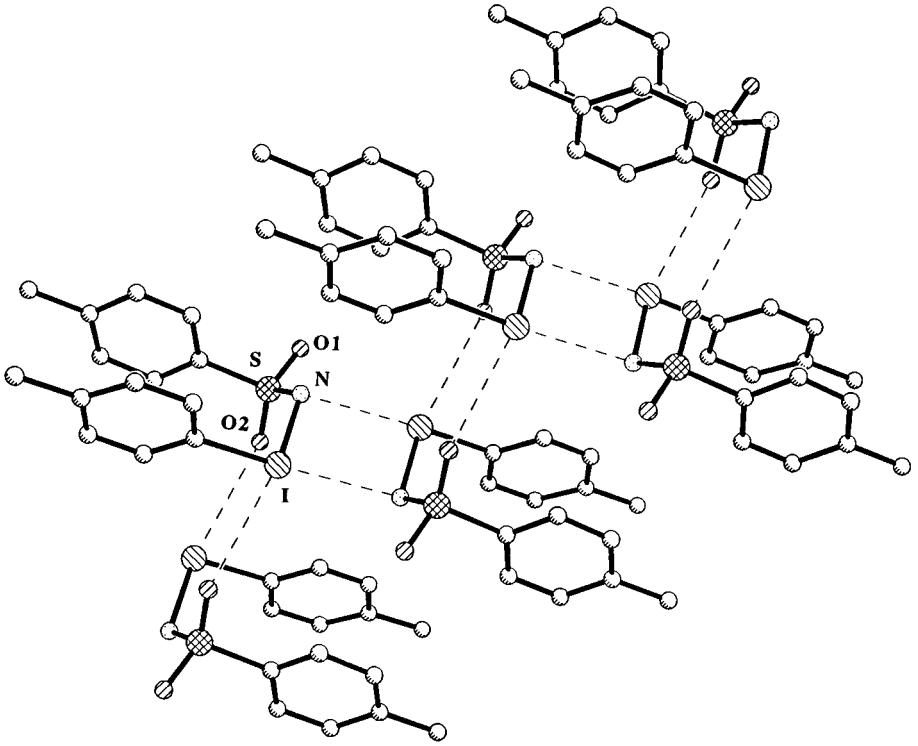

Figure 9. Solid-state aggregation of **4** with polymeric stepladders running parallel to the *b* axis. Hydrogen atoms have been omitted for clarity.

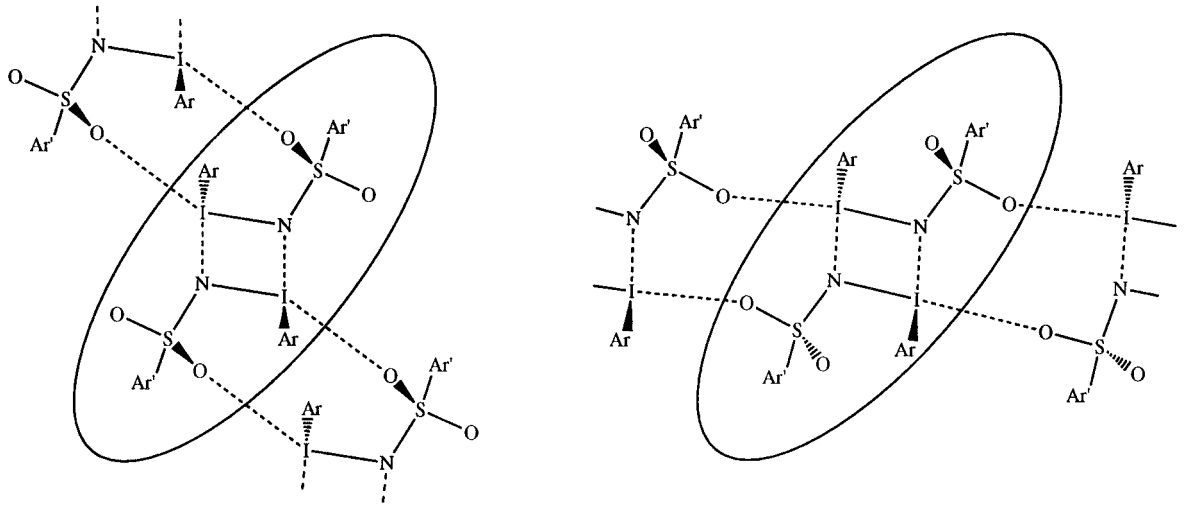

Figure 10. Comparison of the I···O secondary bonds used in construction of linear ladder structure of *o*-TolylINTs and the stepladder structure of *p*-TolyINTs (**4**).

onstrated that application of this expression (using $\beta = 0.09$) gives a "corrected" I−N single bond distance of 1.99 Å, in near agreement with observed data for PhINTs and MesINTs.[46] This formula, thus, is able to make adjustments for differences in electronegativities between two elements bound to one another. The current bond, if truly a single bond, places substantial charges of equal and opposite sign on the I and N atoms, and increases the necessity of corrections of the type that eq 4 imposes. Crystallographic investigations of three-coordinate T-shaped $PhIX_2$ species, however, often reveal lengthened bonds to the two mutually *trans* ligands (typically longer than the sum of covalent radii) and, thus, obliviate the need for electronegativity corrections. Near-normal single bond lengths can be realized for one of the two ligands in cases where a substantial difference exists in electronegativity of the two X groups.[9] These two ligands share bonding to a single p-orbital on the central atom (forming a three-center, four-electron bond), which leads to longer and weaker bond strengths. Little disparity is found in the two I−X bond lengths for solid-state halonium ion dimers of the form $[Ar_2IX]_2$.[2] In the present compounds, the second axial site is satisfied by secondary bonding to a neighboring nitrogen or oxygen atom which has little effect on disrupting I−N bonding. Lacking this competition for an iodine p orbital, the $NSO_2Ar'^{2-}$ ligand can maximize I−N bonding. The coordination geometry about each iodine(III) center must account for secondary bonding contacts and, thus, will be discussed in conjunction with the nature of the solid-state aggregations (below).

The nature of the bonding in $ArINSO_2Ar'$ has also been studied by *ab initio* calculation (STO 3-21G* level) levels using crystallographic data for MesINTs (chosen as it contains the

(69) For discussion regarding problems with eq 4, see: (a) Wells, A. F. *J. Chem. Soc.* **1949**, 55−67. (b) Wells, A. F. *Structural Inorganic Chemistry*, 5th ed.; Oxford University Press: London, 1984.

Table 3. Intramolecular Structural Comparisons for $XC_6H_4INSO_2C_6H_4Y$

	X, Y							
distances (Å) and angles (deg)	H,[a,b] *p*-CH_3	*o*-CH_3,[c] *p*-CH_3	*o*-CH_3,[c,d] *p*-CH_3	*m*-CH_3,[e] *p*-NO_2 (**1**)	*m*-CH_3,[e] *p*-CH_3 (**2**)	*m*-CH_3,[e] H (**3**)	*p*-CH_3,[e] *p*-CH_3 (**4**)	1,3,5-Me_3,[a] *p*-CH_3
I−N	2.039(2)	2.011(2)	2.013(3)	2.012(3)	2.005(5)	1.997(8)	2.009(4)	2.008(4)
I−C1	2.110(3)	2.114(3)	2.107(3)	2.104(4)	2.104(5)	2.101(8)	2.113(4)	2.119(4)
N−S	1.611(2)	1.604(3)	1.601(4)	1.589(3)	1.610(5)	1.611(7)	1.622(4)	1.595(4)
I···O	[3.139]	3.278	3.235	3.278	3.221	3.250	3.255	3.227
C1-I−N	95.8(1)	100.3(1)	98.7(1)	99.3(1)	100.8(2)	100.6(3)	102.1(2)	102.2(1)
I−N−S	117.4(1)	114.1(1)	111.4(2)	114.6(2)	111.3(3)	116.4(4)	114.4(2)	114.5(2)
N−I−C1-C2	[−67.2]	69.8(2)	88.3(3)	103.6(3)	84.8(5)	−61.4(8)	82.5(4)	−109.7
N−I−C1-C6	[110.0]	−109.6(2)	−91.2(3)	−74.2(3)	−95.6(5)	119.1(8)	−95.8(4)	67.9
C1−I−N−S	[83.1]	75.2(2)	−108.0(2)	−80.2(2)	−110.1(3)	−62.7(5)	78.0(2)	71.2
I−N−S−C	[−106.4]	−77.5(2)	71.7(2)	78.1(2)	72.5(3)	86.3(5)	−80.4(3)	−82.9
angle between rings[f]	[47.1]	9.78(5)	43.38(9)	6.1(2)	47.7(1)	4.5(3)	11.6(2)	19.6
distance between rings[g]	[4.614]	3.57	4.51	3.59	4.74	3.60	3.82	3.82

[a] Reference 46. [b] Values in brackets are from reference 47. [c] Reference 48. [d] Second polymorph B. [e] This work. [f] Using least-squares planes through six carbon atoms. [g] Centroid-to-centroid distance.

Table 4. Natural Bond Orbitals Analysis of the Valence Bonds about $PhINSO_2Ph$ Core

bond	occupancy	contribution (%)	hybrid composition
I−C	1.98	I, 38	$sp^{5.5}$ (s, 15%; p, 84%)
		C, 62	$sp^{2.8}$ (s, 36%; p, 64%)
I−N	1.97	I, 39	$sp^{5.5}$ (s, 15%; p, 84%)
		N, 61	$sp^{4.0}$ (s, 20%; p, 80%)
N−S	1.97	N, 64	$sp^{2.7}$ (s, 27%; p, 73%)
		S, 36	$sp^{3.5}$ (s, 22%; p, 77%)
S−O1	1.98	S, 35	$sp^{2.5}$ (s, 28%; p, 70%)
		O, 65	$sp^{3.2}$ (s, 24%; p, 76%)
S−O2	1.98	S, 34	$sp^{2.9}$ (s, 25%; p, 73%)
		O, 66	$sp^{3.4}$ (s, 22%; p, 78%)
S−C	1.96	S, 43	$sp^{2.9}$ (s, 25%; p, 73%)
		C, 57	$sp^{2.8}$ (s, 27%; p, 73%)
N, LP1	1.96	N, 100	sp (s, 50%; p, 50%)
N, LP2	1.82	N, 100	p (s, 3%; p, 97%)
I, LP1	1.99	I, 100	$sp^{0.43}$ (s, 67%; p, 29%)
I, LP2	1.96	I, 100	p (s, 0.5%; p, 99.5%)

"least" degree of intermolecular association) to generate monomeric $PhINSO_2Ph$ for computational study. There are a total of 87 occupied molecular orbitals, both core and valence, derived from the calculation. Besides the core orbitals, most low-energy valence orbitals can be assigned to C−H, C−C, S−O, and S−N σ bonds and C−C π bonds, which are less relevant to our interest and, hence, omitted from future discussion. Due to the lack of molecular symmetry, only a less rigorous qualitative analysis of the bonding scheme is presented. Extended Hückel and CNDO/2 calculations have appeared for $PhICl_2$ and $PhIF_2$, which are more readily interpreted owing to the higher symmetry in these species.[70]

Among the MOs of interest, both the HOMO and SHOMO (second-highest occupied MO) are attributed to the π bonding orbitals localized on the phenyl rings, with the former containing a small contribution of the nitrogen atom. The LUMO (MO 88) appears to be the combination of the σ^*(I−N) orbital and the π^* orbital of the phenyl group attached to iodine. Thus, the ability of $ArINSO_2Ar'$ to act as efficient nitrene delivery systems may be related to a readily accessible LUMO. While both the low molecular symmetry and the delocalized nature of most upper valence MOs prohibit a clear analysis of covalent bonding scheme around the $PhINSO_2Ph$ core from the composition of the molecular orbitals, such an analysis is available through the so-called natural orbital analysis.[56,71] The result for the key bonds is tabulated in Table 4. It is clear from this table that the core is supported by C−I, I−N, N−S, and S−C single bonds. This scheme reinforces the above analysis of the structural data which speak out against the presence of an I═N bond. Furthermore, the presence of a total S−O bond order of two as opposed to three or four indicates that both S−O bonds are dative in nature, which implies a significant build-up of positive charge on the S center and negative charge on O centers. Consistently, Mülliken population analysis places formal charges of +0.91, −0.88, +1.66, −0.59, and −0.70 on I, N, S, O1, and O2 centers, respectively. On the basis of both the natural bond orbital analysis and the charge distribution, the following canonical structures are proposed, with the structure on the left being the most stable.

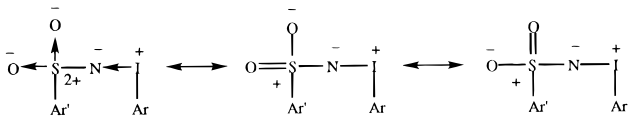

Ar−I Bonds. Structurally characterized carbene adducts of aryl iodides ($PhICR_2$) can be contrasted to the nitrene adducts, $ArINSO_2Ar'$.[3,9,72] These species display I−C(carbene) bond lengths in the range of 2.039−2.13 Å, and the values for the I−C(phenyl) bonds within these materials fall between 2.07 and 2.104 Å. The close relationship between the two sets of data imply little, if any, I−C multiple bonding. The mean value for aryl−iodide bond lengths is 2.095 Å, suggesting that addition of the nitrene to the aryl iodide in $ArINSO_2Ar'$ does little to perturb the Ar−I bond.[73] This result is also in accord with the view that oxidation minimally detracts the iodine s orbital involvement in bonding to the aryl residue. The angles about each iodine atom in the compounds from Table 3 range from 95.8(1) to 102.2(1)°. Angles about the nitrogen atoms (I−N−S) show little variance and span 111.4(2)−117.4(1)°.

N−SO_2Ar' Bonds. The N−S distances observed (1.595(5)−1.619(3) Å) are somewhat shorter than that predicted by the use of eq 4 (1.69 Å). It has been suggested that this observation indicates partial N−S multiple bonding in these and other species.[46] The results of our calculations presented above suggest only N−S single bonding. Examination of S−N distances in related sulfur ylides of the form R_2SNSO_2R' reveal longer R_2S−N bonds than N−SO_2R bond lengths. For example, the S(IV)−N bond length of 1.628(7) Å is 0.03 Å longer than the corresponding S(VI)−N bond length of 1.598(7) Å in Ph_2-

(70) Mylonas, V. E.; Sigalas, M. P.; Katsoulos, G. A.; Tsipis, C. A.; Varvoglis, A. G. *J. Chem. Soc., Perkin Trans. 2* **1994**, 1691−1696.
(71) Reed, A. E.; Curtiss, L. A.; Weinhold, F. *Chem. Rev.* **1988**, *88*, 899−926.
(72) Moriarty, R. M.; Prakash, I.; Prakash, O.; Freeman, W. A. *J. Am. Chem. Soc.* **1984**, *106*, 6082−6084.
(73) Bürgi, H.-B.; Dunitz, J. D. *Structure Correlation*; VCH: New York, 1994; Vol. 2.

SNTs. Resonance structures could be drawn for multiple bonding between each pair of S and N atoms. Alternatively, the S−N bonds might also be shortened by ionic effects (see below).

Intramolecular I···O Bonding. All the $ArINSO_2Ar'$ structures described above adopt a "U-turn" structural motif. As discussed further below, this arrangement places the two aryl residues near one another. Weak intramolecular I···O bonds occur in each $ArINSO_2Ar'$ structure (not depicted in figures, for clarity) and span the narrow range of 3.139−3.278 Å. Intramolecular I···O bonding is common in species such as $ArI(O_2CR)_2$.[3] Further discussion of I···O bonding is provided below. The particular arrangement of I···O intramolecular bonding probably aids in guidance to formation of the U-turn motifs (below), but, owing to the location of the oxygen atom

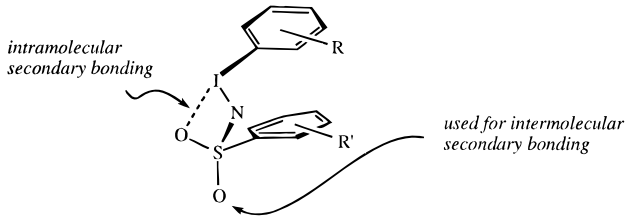

contact within the coordination sphere of the iodine atom and the constraints of the four-membered ring, this interaction is probably weak. This notion is corroborated by the longer intramolecular I···O distances relative to the intermolecular I···O distances. Additionally, rotation about the I−N bond by 180° can yield an alternative structure whereby the two aryl residues are directed away from one another (and, presumably, yield a less crowded molecule) and yet achieve the same intramolecular I···O contact distance. This orientation, however, may discourage intermolecular I···N bonding.

Solid-State Polymers and I···X Secondary Bonding. The iodine−nitrene ylides constitute unique members of a bent geometry AX_2E_2 class of compounds, and their complex patterns of secondary bonding can be discussed using nomenclature originally developed for Sb(III) halides.[74] A review of secondary I···O bonding in organoiodine(III) complexes (AX_3E_2) has shown that I···O secondary bonds as short as 2.768(8) Å can be realized.[75] Although an exact assessment of I···O and I···N attractive forces is somewhat difficult, comparisons of the I···O and I···N bond distances can be made to the corresponding sum of the van der Waal radii (I, 1.96, N, 1.55, and O, 1.50 Å).[76] Distances shorter than 3.51 Å for I···N and 3.46 Å for I···O bonds thus indicate some degree of interaction. Interestingly, *N*-iodosuccinamide contains extremely short (2.580(6) Å) I···O secondary bonds (relative to the longer Br···O secondary bond distance of 2.88 Å in *N*-bromosuccinamide).[63] Structural investigations of halonium ions, such as [PhI(C≡CR)]OTf, have shown that weak association of the triflate completes a formally T-shaped geomtery (ψ-TBP) at the iodine centers, and such interactions (I···O) occur at distances that range from 2.56 to 2.62 Å.[2] Furthermore, secondary C−I···X (X = N, O) interactions are also not limited to organoiodine(III) species, and metrical preferences for other oxidation states have been described.[77−79]

The structures of most commonly observed organoiodine(III) AX_3E_2 molecules, including secondary bonds, may be

Chart 1

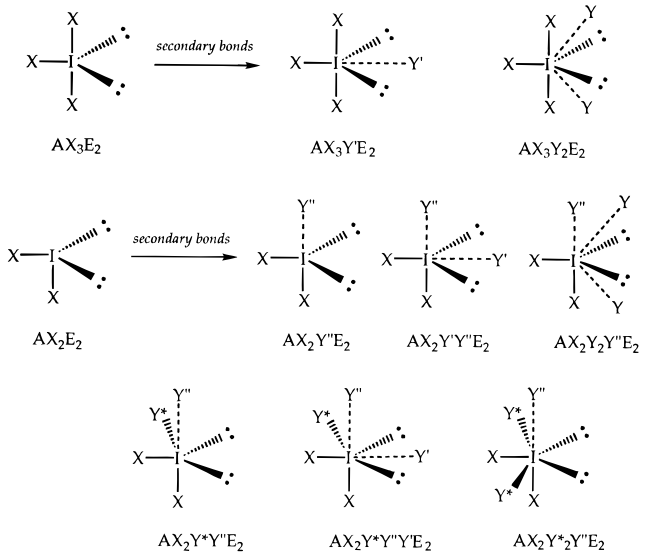

considered as pseudo-trigonal-bipyramidal (ψ-TBP) species either having one such contact in between the E···E edge to form a $AX_3Y'E_2$ geometry (see Chart 1) or having two secondary bonds located between the X···E edges to form a $AX_3Y_2E_2$ geometry. Extension of this analysis to the present case is also illustrated in Chart 1 (Y″ is used to recognize a secondary bond *trans* to the more electronegative nitrogen atom). For comparative purposes, structural representations of the solid-state structures for PhINTs, *o*-TolylINTs, and MesINTs are presented in Chart 2. Under this nomenclature, the structures of $ArINSO_2Ar'$ (except MesINTs) can be assigned. Owing to the relatively open nature of the AX_2E_2 core geometry and the increased charges on the iodine and nitrogen, more extensive aggregations are expected and are realized. Details of the nature and arrangements of the critical secondary bonds in the $ArINSO_2Ar'$ series are summarized in Table 5. The parent species, PhINTs, is unique and adopts a packing to achieve $AX_2Y''E_2$ geometry using predominantly secondary I···N bonding, directed *trans* to the nitrogen atom within PhINTs. In nearly all of these structures, the shortest secondary bonds are located in the apical position (designated as Y″), which completes a ψ-TBP structure.

In the structure of *o*-TolylINTs (polymorph A), secondary bonding by a sulfonyl oxygen atom is found to occupy the Y″ site. A longer secondary bond to a neighboring nitrogen atom at a Y′ site completes the observed $AX_2Y''Y'E_2$ geometry. The second polymorph of *o*-TolylINTs (B) does not have this second interaction and is best described as a $AX_2Y''E_2$ geometry. The weakness of the I···N secondary bonds in *o*-TolylINTs is indicated not only by the long I···N distances (3.140 Å) but also by the coexistence of the two polymorphs.

Compound **1** uses two I···O contacts and one I···N contact and can be described as a geometry based on $AX_2Y_2Y''E_2$. The sulfonyl oxygen atom not employed in intramolecular I···O bonding finds itself bridged to two iodine atoms. Addition of I···N bonding transforms a single linear chain such as that found in *o*-TolylINTs (B) into the two-dimensional sheetlike structure in **1**. Essential to this conversion is significant rotation about the I−N bonds to interchange between the two structures (see Table 3 and C−I−N−S torsion angles).

Compound **2** uses I···O secondary bonds in the Y″ site and long (and presumably weaker) I···N bonds. The location of

(74) Sawyer, J. F.; Gillespie, R. J. *Prog. Inorg. Chem.* **1986**, *34*, 65−113.
(75) Batchelor, R. J.; Birchall, T.; Sawyer, J. F. *Inorg. Chem.* **1986**, *25*, 1415−1420.
(76) Bondi, A. *J. Phys. Chem.* **1964**, *68*, 441−451.
(77) Ramasubbu, N.; Parthasarathy, R.; Murray-Rust, P. *J. Am. Chem. Soc.* **1986**, *108*, 4308−4314.
(78) Murray-Rust, P.; Motherwell, W. D. S. *J. Am. Chem. Soc.* **1979**, *101*, 4374−4376.
(79) Cody, V.; Murray-Rust, P. *J. Mol. Struct.* **1984**, *112*, 189−199.

Chart 2

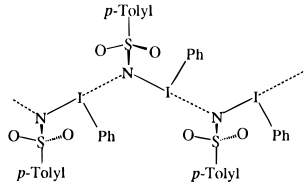

PhINTs

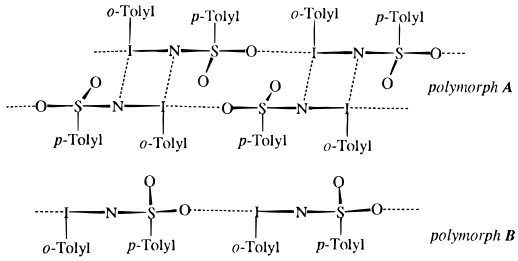

***o*-TolylINTs**

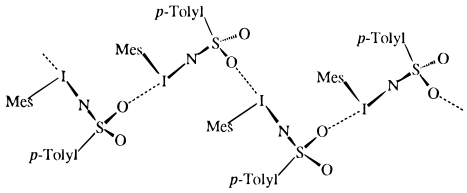

MesINTs

the I···N interactions is such that the molecule is better described as portrayed in Chart 1 as $AX_2Y''Y^*E_2$ (Y* being a site ~90° to the C−I bond and located approximately perpendicular to the plane of AX_2Y'' atoms).

Compound **3** is closely related to *o*-TolylINTs (polymorph A) but containing an additional I···O interaction and is best described by an $AX_2Y''Y'YE_2$ geometry. The geometry for **4**, however, is intermediate to the above structures. The expected stronger interaction *trans* to the I−N bond is displaced by about 30° and is occupied by a weaker I···O interaction (3.191 Å). A much longer distance of 3.563 Å (not indicated on Figure 9), spanning O1 and an iodine atom, can also be discerned. An exact assignment of **4** to one of the structural forms in Chart 1 is somewhat difficult. The structure most closely fits a AX_2-$YY^*Y''E_2$ geometry.

It has been noted that hydrogen bonding forces may rival those of I···O secondary bonding forces.[75] In the series of compounds, the closest C−H···O and C−H···N contacts are 2.37 and 2.62 Å (for *o*-TolylINTs, polymorph A, and **3**, respectively). Hydrogen bonding in this set of compounds thus plays a rather minor role in aggregation.

Aryl−Aryl Interactions. An interesting feature of all the ArINSO$_2$Ar′ structures is the "U-turn" structural motif adopted by the monomeric units. This arrangement places the two aryl residues in somewhat close proximity to one another (see Table 3) and suggests a role for attractive aryl−aryl interactions in the solid-state structures of ArINSO$_2$Ar′. Alternatively, the aryl residues may be forced into this arrangement by the desire of the monomers to bare their highly charged atoms (I, N, S, and O) onto a single side for maximal engagement to atoms of opposite charge, thus affording maximal intermolecular secondary bonding. Attractive forces between aromatic moieties have been recognized as an important structural feature in many systems and various methods have been used to assay the strength of such interactions.[80−84] Two aromatic rings can enjoy stabilizing van der Waals attractions by arranging themselves in varying orientations to one another. The most commonly observed (and discussed) geometrical arrangements are ones involving face-to-face interactions (or π stacking) and those based on a T-shaped geometry. The latter geometry directs an aromatic C−H bond at the π cloud of another aromatic ring. Calculations for the benzene dimer favor the T-shaped geometry, while corresponding calculations for the toluene dimer favor a displaced sandwich arrangement.[81] In general, attractive π stacking forces are probably most significant when the centroid-to-centroid distance approaches 3.4−3.5 Å and can yield a maximal stabilization of about 2−2.5 kcal/mol. For the T-shaped geometries, a centroid-to-centroid distance of 5 Å can yield similar stabilization energies. Data in Table 3 indicate that, in *o*-TolylINTs (polymorph A), **1**, **3**, **4**, and MesINTs, the aromatic residues are roughly coplanar, with centroid-to-centroid distances ranging from 3.57 to 3.82 Å. The aromatic rings are clearly noncoplanar in PhINTs, *o*-TolylINTs (polymorph B), and **2** and afford centroid-to-centroid distances of 4.51−4.74 Å. Intermolecular Ar···Ar interactions are less evident in **1**−**4**.

I···Aryl Interactions. Table 5 reveals a notable lack of secondary interactions for MesINTs. This material contains the most sterically demanding aryl group of the series, but, like all other ArINSO$_2$Ar′, the molecule still adopts the U-turn shape in the solid-state. The structure uses short I···O secondary bonds at the Y″ sites and, on first approximation, could be assigned a $AXY''E_2$ geometry. However, upon closer inspection, the Y site seems to be occupied by an intermolecular secondary bonding to the mesityl ring of a neighboring unit of MesINTs (below). The centroid-to-iodine distance is 3.46 Å,

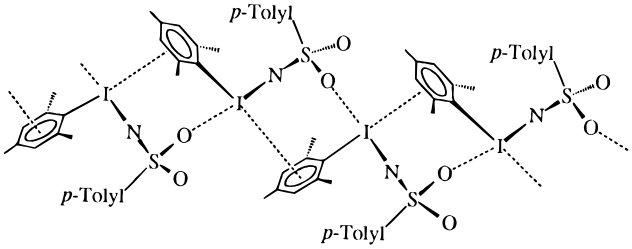

and below the sum of the covalent radii for the groups (~3.66 Å). The centroid−I−C and centroid−I−N angles are 142.6 and 98.0°, respectively. Ample evidence for charge transfer complexes between I_2 and arenes exists.[85] In MesINTs the iodine atom appears to balance some of the electropostive charge by interactions with the electron-rich mesityl rings. The structure is thus highly packed by the unique nature of the cyclic array formed. The structure of Br_2·benzene has been determined, and the bromine-to-centroid distance is 3.36 Å.[85]

Comparisons to *N*-sulfonylimides of group VI elements of the form R_2XNSO_2R' (X = S, Se, Te) provide some interesting contrasts and some additional insights into the structures of ArINSO$_2$Ar′.[86−91] These ylides, of course, have one more organic group and one less lone pair than the corresponding iodine(III) N-ylides. The additional organic groups make the hypervalent atoms in these ylides more sterically protected and

(80) Sun, S.; Bernstein, E. R. *J. Phys. Chem.* **1996**, *100*, 13348−13366.
(81) Chipot, C.; Jaffe, R.; Maigret, B.; Pearlman, D. A.; Kollman, P. A. *J. Am. Chem. Soc.* **1996**, *118*, 11217−11224.
(82) Dahl, T. *Acta Chem. Scand.* **1994**, *48*, 95−106.
(83) Hobza, P.; Selzle, H. L.; Schlag, E. W. *Chem. Rev.* **1994**, *94*, 1767−1785.
(84) Hunter, C. A. *Chem. Soc. Rev.* **1994**, 101−109.
(85) Hassel, O.; Rommong, C. *Q. Rev., Chem. Soc.* **1962**, *16*, 1−18.

Table 5. Details of Major Secondary Bonding in $XC_6H_4INSO_2C_6H_4Y$

distances (Å) and angles (deg)	X, Y: H,[a] *p*-CH_3	*o*-CH_3,[b] *p*-CH_3	*o*-CH_3,[b,c] *p*-CH_3	*m*-CH_3,[d] *p*-NO_2 (**1**)	*m*-CH_3,[d] *p*-CH_3 (**2**)	*m*-CH_3,[d] H (**3**)	*p*-CH_3,[d] *p*-CH_3 (**4**)	1,3,5-Me_3,[a] *p*-CH_3
I···N	2.482 (Y″)	3.140		3.073	2.992	2.933	3.132	
I···O		2.849 (Y″)	2.826 (Y″)	2.971 (Y″)	2.863 (Y″)	2.975 (Y″)	3.191	2.857
I···O′				3.361				
N−I···N	177.8	77.95		85.8	105.7	73.1	77.3	
N−I···O		170.23	168.7	167.2	176.4	167.4	149.6	171.2
N−I···O′				122.5		110.8	112.2	
C−I···O		78.6	76.8	75.4	78.4	74.9	78.8	75.7
C−I···O′				137.7		141.7	136.2	
C−I···N	83.0	178.2		161.8	89.9	173.7	175.1	

[a] Reference 46. [b] Reference 48. [c] Second polymorph B. [d] This work.

discourage aggregation in the solid-state, and they also make these materials more soluble in organic media. Most noticeable is the lack of any consistent orientation of the aryl residues among the structures containing aryl residues on both halves of the molecules; this suggests that aromatic π stacking forces play little role in intramolecular structures of the chalcogen N-ylides.

These ylides are also less extensively aggregated in the solid-state than their iodine(III) counterparts, owing to, perhaps less formal charges on the chalcogen and nitrogen atoms. As mentioned above, the R_2S-N bond (1.628(7)−1.636(8) Å) in R_2SNSO_2R' is *longer* than the $N-SO_2R'$ bond. The greater charge on the S(VI) over that of the S(IV) atom seems to lead to the observed decreased bond lengths. Interestingly, for the example of a structurally characterized tellurium *N*-sulfonyl ylide, the Te−N bond length is found to be shorter than the I−N bond lengths described above (1.980(3) Å), even though the Te covalent radius (1.35 Å) is 0.02 Å larger than that of iodine (1.33 Å). Using corrections for ionicity in the X−N bond (eq 4), differences in the electronegativities between I (2.66 Å) and Te (2.10 Å) apparently counterbalance differences in the covalent radii between these elements and lead to predicted I−N and Te−N distances of 2.06 and 2.00 Å.

Conclusions

The primary nitrene sources $ArINSO_2Ar'$ have been shown by us and others to simultaneously show similarity and diversity in their solid-state structures. All of the materials characterized thus far contain I−N bond lengths that fall within the narrow range of 1.997(8)−2.039(2) Å. Analysis of the structural and calculational data suggests little evidence for I−N multiple bonding. Resonance forms placing substantial amounts of charge on the I, N, S, and O atoms are consistent with *ab initio* calculations and the nature of the aggregation of the monomers of $ArINSO_2Ar'$. The two sets of aryl residues in these compounds are found to reside on the same half of each monomer and give rise to a U-turn shape for the molecules. For each of the six different $ArINSO_2Ar'$ species structurally characterized (and the resulting seven structural determinations), a different packing is found in the solid-state. Each material uses I···N or I···O secondary bonding (or a combination of both) to wed the monomers into various supramolecular arrays of zig−zag polymers, linear polymers, layered structures, two-dimensional ladders, and three-dimensional stepladders. Some of these materials also use I···arene secondary bonding and combinations of π stacking to achieve these novel and complicated structures. Current work is addressed at determining the relationships between these structures and solution behavior and reactivity.

Acknowledgment. We thank the CWRU Department of Chemistry and the donors of The Petroleum Research Fund, administered by the ACS, for support of this work. The computational facility at Florida Tech is supported by NSF (DUE9350995).

Supporting Information Available: Full crystallographic details for **1**−**4** and details of computational studies of $PhINSO_2$-Ph (24 pages). See any current masthead page for ordering and Internet access instructions.

JA971048O

(86) Kálmán, A.; Duffin, B.; Kucsman, Á. *Acta. Crystallogr.* **1971**, *B27*, 586−594.
(87) Cameron, A. F.; Hair, N. J.; Morris, D. G. *J. Chem. Soc., Perkin Trans. 2* **1973**, 1951−1954.
(88) Roesky, H. W.; Weber, K.-L.; Seseke, U.; Pinkert, W.; Noltemeyer, M.; Clegg, W.; Sheldrick, G. M. *J. Chem. Soc., Dalton Trans.* **1985**, 565−571.
(89) Furmanova, N. G.; Naddaka, V. I.; Krasnov, V. P. *Zh. Strukt. Khim.* **1984**, *25*, 166−169.
(90) Kálmán, A. *Acta. Crystallogr.* **1967**, *22*, 501−507.
(91) Furmanova, N. G.; Gerr, R. G.; Krasnov, V. P.; Naddaka, V. I. *Zh. Strukt. Khim.* **1981**, *22*, 118−122.